OXIDATION OF SULFUR COMPOUNDS
IV: THE PHOTO-OXIDATION OF CH₃SH

R. JEFFREY BALLA and JULIAN HEICKLEN

Department of Chemistry and Center for Air Environment Studies, The Pennsylvania State University, University Park, PA 16802 (U.S.A.)

Summary

The photo-oxidation of CH_3SH has been studied at 296 ± 1 K by both direct photolysis of CH_3SH at 253.7 nm and photolysis of $(CH_3S)_2$ above 280 nm in the presence of CH_3SH and O_2. The direct photolysis of CH_3SH in the presence of O_2 produces H_2, SO_2, H_2S, $CH_3SCH_2SCH_3$ and $(CH_3S)_2$ as products. When $(CH_3S)_2$ is photolyzed in the presence of CH_3SH and O_2, no H_2, SO_2 or H_2S is observed but $CH_3SCH_2SCH_3$ is produced. Thus the formation of H_2, SO_2 and H_2S does not come from CH_3S oxidation but is associated with the hydrogen atom produced in the photolysis of CH_3SH, while $CH_3SCH_2SCH_3$ comes from the oxidation of CH_3S radicals.

The competition for hydrogen atoms by CH_3SH and O_2 via the reactions

$$H + CH_3SH \longrightarrow H_2 + CH_3S \qquad (17)$$

$$H + O_2 + M \longrightarrow HO_2 + M \qquad (20)$$

was measured from both the H_2 and the SO_2 yields. The ratio k_{17}/k_{20} is $(1.07 \pm 0.09) \times 10^{-3}$ $Torr^{-1}$ with O_2 as a chaperone from the H_2 data, and about the same value is obtained from the SO_2 data. If k_{20} is taken as $(5.5 \pm 0.5) \times 10^{-32}$ cm^6 s^{-1}, then k_{17} is about $(1.8 \pm 0.2) \times 10^{-12}$ cm^3 s^{-1}.

From isotopic substitution measurements it was shown that $CH_3SCH_2SCH_3$ was produced from two CH_3S radicals and one CH_3SH molecule. $C_3H_8S_2$ is not formed directly from CH_3S since its formation requires the presence of O_2, but may be produced from both $CH_3S(O)_2$ and CH_3SO_4 radicals reacting with CH_3SH.

It was also seen that CD_3S and the oxygenated CD_3S radicals can exchange with $(CH_3S)_2$ to give CH_3SSCD_3.

1. Introduction

In our earlier work on the photolysis of $(CH_3S)_2$ in the presence of O_2 at 253.7 nm and 296 K [1] we showed that O_2 adds rapidly to CH_3S, and that the oxidation can be explained by the mechanism

$$CH_3S + O_2 \longrightarrow CH_3SOO \qquad\qquad (1)$$

$$CH_3SOO \longrightarrow CH_3S(O)_2 \qquad\qquad (2)$$

$$CH_3SOO + O_2 \longrightarrow CH_3SO_4 \qquad\qquad (3)$$

$$CH_3SO_4 \longrightarrow HO + CH_2O + SO_2 \qquad\qquad (4)$$

$$CH_3SO_4 + (CH_3S)_2 \longrightarrow \text{termination} \qquad\qquad (5)$$

The rate coefficients k_2/k_3 and k_4/k_5 were found to be 110 ± 24 Torr and 0.98 ± 0.19 Torr respectively. In this paper we extend these studies to the photo-oxidation of CH_3SH.

2. Experimental details

The experimental procedure was similar to that described in our earlier reports [1 - 3]. Photolysis of CH_3SH at 253.7 nm and 296 ± 1 K took place in the reaction system used for $(CH_3S)_2$ photo-oxidation [1].

A few experiments were performed in a 631 ml spherical quartz cell equipped with Pyrex–quartz graded seals which contributed no more than 4% to the dead volume. One unfiltered low pressure Hanovia mercury lamp of the type described earlier [1] was used.

Some runs were done in which $(CH_3S)_2$ was photolyzed in the presence of CH_3SH or CD_3SH. This could be done because $(CH_3S)_2$ absorbs light slightly beyond 300 nm, while the extinction coefficients for CH_3SH and CD_3SH are negligible above 275 nm. In these experiments three Hanovia medium pressure type SH U-shaped mercury lamps were used with two Corning 0-53 filters to remove radiation with wavelengths below 280 nm. To be certain that CH_3SH was not absorbing any radiation an experiment was performed in which pure CH_3SH was irradiated; no $(CH_3S)_2$ was found. All experiments of this type were performed in the 631 ml quartz bulb.

Continuous product analysis was performed by allowing the contents of the cell to bleed through a small pinhole into an Extranuclear type II quadrupole mass spectrometer. In the course of these experiments the total pressure in the cell ranged from 20 to 300 Torr. In order to maintain the operating pressure of the mass spectrometer below 4×10^{-6} Torr a series of three glass pinholes of different area were used. The glass pinholes were used over the following total pressure ranges: 20 - 60 Torr, 60 - 150 Torr and 150 - 350 Torr. Under all experimental conditions, sample depletion never exceeded 5%. Mass spectrometric determinations were performed with 40 eV electrons by measuring the product ion current peaks relative to the m/e 40 peak from a known amount of argon which was added to the mixture prior to irradiation. This reduces errors from instrumental or other fluctuations. $(CH_3S)_2$ and bis(methylthio)methane $((CH_3S)_2CH_2)$ were quantitatively determined by measuring their signals at m/e 94 and m/e 108 respectively relative to that of argon at m/e 40. The mass spectral sensitivity of

deuterated compounds, except for CD_3SH which could be measured directly, was assumed to be the same as for their protonated analogs. This introduces some error as the relative sensitivity of CH_3SH and CD_3SH is 0.86.

H_2, SO_2, CH_4 and H_2S were analyzed using gas chromatography. After termination of irradiation, the contents of the reaction vessel were expanded into two sample loops. From one loop, H_2 or CH_4 was analyzed. CH_4 was analyzed on a column 6 ft long and 1/4 in in diameter containing molecular sieve 5A. Helium was used as a carrier gas with a flow rate of 45 ml min^{-1}. In order to prevent column contamination, all materials which would not pass through the column were retained in the sample loop by immersing it in liquid nitrogen. The separation of H_2 was performed on a stainless steel column 12 ft long and 1/4 in in diameter containing molecular sieve 5A maintained at room temperature. Nitrogen was used as the carrier gas with a flow rate of 40 ml min^{-1}. All gases which would not pass through the column were retained in the sample loop using an isopentane slush bath maintained at 113 K. SO_2 and H_2S were analyzed from the second loop; the loop was cooled to 77 K and all non-condensable gases were evacuated. A chloroform slush bath (210 K) was used to retain low vapor pressure compounds in the sample loop. The volatile compounds at this temperature were injected onto an FEP Teflon column 13 ft long and 3/16 in in diameter containing GP20% SP-2100/0.1% Carbowax 1500 on 100/120 Supelcoport at room temperature.

CH_3SH (minimum purity, 99.5%), obtained from Matheson, was further purified using trap-to-trap vacuum distillation from 179 to 113 K. Methane-d_3-thiol (CD_3SH) (minimum purity, 99 at.%) was obtained from MSD Isotopes. It was purified using the procedure described for CH_3SH. Red label $(CH_3S)_2$, obtained from Aldrich, was distilled from 273 to 210 K. Bis-(methylthio)methane (minimum purity, 99%), obtained from Aldrich, was not distilled but was thoroughly degassed prior to use. Anhydrous SO_2 (Matheson) was distilled from 179 to 142 K. Prepurified grade nitrogen (minimum purity, 99.998%) and extra dry grade oxygen (minimum purity, 99.6%) were obtained from MG Scientific Gases. Prepurified hydrogen (purity, 99.95%) and prepurified argon (purity, 99.998%) were obtained from Matheson. The nitrogen, oxygen, hydrogen and argon were used without further purification.

C.P. grade methane (minimum purity, 99.0%), obtained from Matheson, was distilled from 87 to 77 K. C.P. grade H_2S (minimum purity, 99.5%), obtained from Matheson was distilled from 142 to 113 K. Tetra-fluoromethane (CF_4) (minimum purity, 99.7%), obtained from Matheson, was distilled from 113 to 77 K and was thoroughly degassed prior to each experiment.

Methyl thionitrite (CH_3SNO) was prepared by photolyzing $(CH_3S)_2$ at 254 nm in the presence of a threefold excess of NO obtained from Matheson. The CH_3SNO was purified by trap-to-trap distillation from 200 to 113 K. The purified material was stored in a darkened storage bulb at 77 K to prevent thermal as well as photolytic decomposition.

Mass spectra of all gases were obtained and were compared with the Environmental Protection Agency–National Institutes of Health mass spectral data base. In all cases no extraneous peaks were obtained.

Actinometry was performed by photolysis of CH_3SH at 253.7 nm. The products obtained (($CH_3S)_2$ and H_2) have quantum yields of $0.99 \pm 0.1(4)$ and $1.00 \pm 0.05(5)$ respectively. In all cases the absorbed intensity I_a obtained from $(CH_3S)_2$ by mass spectrometry and from H_2 by gas chromatography agreed within a few per cent.

In experiments where $(CH_3S)_2$ was photolyzed in the presence of CH_3SH or CD_3SH, actinometry was performed by photolyzing $(CH_3S)_2$ in the presence of NO and measuring the CH_3SNO produced assuming $\Phi(CH_3SNO) = 2.0$ [2].

In these studies a product occurred at m/e 108. It was identified by a gas chromatography–mass spectrometry technique. A sample was prepared by photolyzing 300 Torr O_2 with 20 Torr CH_3SH and condensing the mixture at 77 K. All reactants including CH_3SH were removed by pumping the mixture at 179 K. At this point only the product with m/e 108 and $(CH_3S)_2$ remained. These substances were injected into a Finnegan 3200 gas chromatography–mass spectrometry system and were analyzed by electron impact. Analysis took place on a glass column 5 ft long with an inside diameter of 2 mm containing 20% SE30 on Supelcoport. Separation was performed isothermally at 383 K using helium as a carrier gas flowing at 20 ml min^{-1}. Afterwards a sample of $(CH_3S)_2CH_2$ (m/e 108) was injected. The mass spectra of the unknown product and $(CH_3S)_2CH_2$ were identical, and their respective retention times differed by only 0.03 min.

In order to be certain about the parent mass of the compound, an experiment similar to that described above was performed using a chemical ionization source. A Finnegan system was used with a batch inlet and with isobutane as the ionizing gas. A signal at m/e 109 was obtained which corresponds to a molecule of mass 108.

3. Results

In the absence of O_2, the photolysis of CH_3SH at 253.7 nm and 296 K gives H_2, $(CH_3S)_2$, CH_4 and H_2S as products. The quantum yields of H_2S and CH_4, which were nearly equal at about 0.18, are essentially independent of reaction time up to 1200 s, indicating that these compounds are primary products of the reaction.

Earlier studies [4, 5] have shown an inert gas pressure effect on the photolysis of CH_3SH. Therefore we studied the reaction in the presence of CF_4. The effect of CF_4 pressure on $\Phi\{(CH_3S)_2\}$ and $\Phi(CH_4)$ in the photolysis of CH_3SH in the absence of O_2 is shown in Table 1. $\Phi\{(CH_3S)_2\}$ remains at 1.00 ± 0.03 independent of pressure, but $\Phi(CH_4)$ drops markedly toward zero as the CF_4 pressure is increased to 763 Torr. The pressure effect on the other two products (H_2 and H_2S) is shown in Table 2. The H_2 yield stays

TABLE 1

Effect of CF$_4$ pressure on CH$_3$SH photolysis[a]

[CF$_4$] (Torr)	I_a (mTorr s^{-1})	$\Phi\{(CH_3S)_2\}$	$\Phi(CH_4)$
0[b]	0.95	1.17	0.196
0	0.89	1.01	0.185
59	0.92	0.97	0.138
108	0.91	0.98	0.111
202	0.67	0.96	0.095
311	0.67	1.03	0.080
492[c]	0.68	—	0.051
509[d]	0.70	—	0.041
763	0.68	—	0.024

[a] [CH$_3$SH] = 20.4 ± 0.7 Torr; [Ar] = 15.0 ± 2.3 Torr; irradiation time, 900 s.
[b] Irradiation time, 610 s.
[c] Irradiation time, 915 s.
[d] [Ar] = 0.

TABLE 2

Effect of nitrogen pressure on CH$_3$SH photolysis[a]

[N$_2$] (Torr)	Irradiation time (s)	I_a (mTorr s^{-1})	$\Phi(H_2S)$	$\Phi(H_2)$
0	900	0.90	0.180	0.95
0	900	0.81	0.214	1.05
0	840	0.79	0.208	1.01
103	973	0.80	0.123	1.16
109	913	0.81	0.134	1.12
308	900	0.85	0.106	1.00
509	900	0.80	0.084	1.14
779	900	0.81	0.086	1.04

[a] [CH$_3$SH] = 21.2 ± 2.2 Torr; [Ar] = 0.

constant at 1.06 ± 0.06 as the inert gas (nitrogen in this case) pressure is increased. However, $\Phi(H_2S)$ is quenched.

CH$_3$SH was photolyzed in the presence of O$_2$ (and argon) at 253.7 nm and 296 ± 1 K. Products of the reaction measured by gas chromatography were H$_2$, H$_2$S and SO$_2$. In addition (CH$_3$S)$_2$ and a product at m/e 108 were monitored by mass spectrometry. The mass spectrum of the product with m/e 108 was obtained by gas chromatography–mass spectrometry and it exactly matched that for CH$_3$SCH$_2$SCH$_3$, including the expected 8% sulfur isotope peak at m/e 110. It gave the same retention time by gas chromatography as authentic samples of CH$_3$SCH$_2$SCH$_3$. Experiments performed with CD$_3$SH shifted the mass spectral peak from 108 to 116, thus indicating that the thiol hydrogen atom is not incorporated into CH$_3$SCH$_2$SCH$_3$.

In order to eliminate the hydrogen atom and its oxygenated analogs from the system, CH_3S radicals were prepared from the photo-oxidation of $(CH_3S)_2$ at wavelengths above 280 nm. When $(CH_3S)_2$ was photolyzed in the presence of CH_3SH and O_2 (and argon), $CH_3SCH_2SCH_3$ was still formed but there was no evidence for H_2, SO_2 or any other product. The absence of SO_2 was very surprising since SO_2 is a major product of the photo-oxidation of either $(CH_3S)_2$ or CH_3SH in the absence of the other. At high O_2 pressures, $CH_3SCH_2SCH_3$ was an initial product of the reaction for CH_3SH photo-oxidation, but at low O_2 pressures there was evidence of an induction period. In the $(CH_3S)_2$ photo-oxidation in the presence of CH_3SH, $CH_3SCH_2SCH_3$ grew with an induction period under all conditions. Typical growth plots for $CH_3SCH_2SCH_3$ are shown in Fig. 1 for the photo-oxidation of both CH_3SH and $(CH_3S)_2$ in the presence of CH_3SH. For those runs that show an induction period for formation, there is also some growth after the termination of irradiation. This behavior suggests that $CH_3SCH_2SCH_3$ might be formed from a long-lived precursor. Quantum yields for $CH_3SCH_2SCH_3$ formation were obtained from the straight-line portion of its growth curve (after the induction period). Experiments also were done in which $(CH_3S)_2$ was photolyzed in the presence of CD_3SH and O_2 (and argon). The 108 mass spectral peak shifted from 108 to 111, thus indicating that only one CD_3SH is involved in
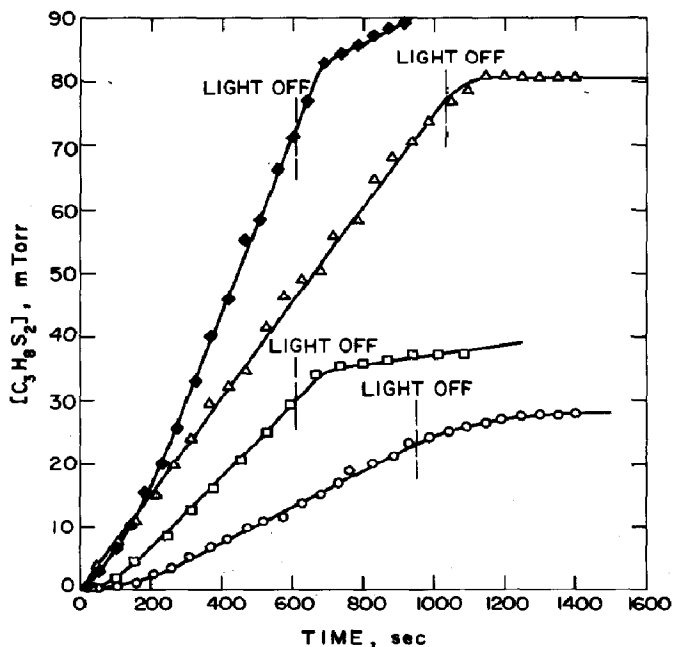

Fig. 1. Plot of $C_3H_8S_2$ pressure *vs.* reaction time during and after photolysis: O, $[CH_3SH] = 21.0$ Torr, $[O_2] = 19.3$ Torr, $[Ar] = 15.8$ Torr and $I_a = 0.48$ mTorr s^{-1}; △, $[CH_3SH] = 21.2$ Torr, $[O_2] = 99.3$ Torr, $[Ar] = 15.0$ Torr and $I_a = 0.48$ mTorr s^{-1}; □, $[(CH_3S)_2] = 8.68$ Torr, $[CH_3SH] = 19.8$ Torr, $[O_2] = 19.9$ Torr, $[Ar] = 14.8$ Torr and $I_a = 0.83$ mTorr s^{-1}; ◆, $[(CH_3S)_2] = 9.47$ Torr, $[CH_3SH] = 25.1$ Torr, $[O_2] = 98.7$ Torr, $[Ar] = 18.8$ Torr and $I_a = 0.71$ mTorr s^{-1}.

its formation. For $(CH_3S)_2$ formation, or its deuterated analogs, there was no induction period or post-irradiation growth under any conditions.

The effect of irradiation time was studied in four series of runs with $[CH_3SH] = 19.6$ Torr and $[O_2]$ values of 20, 62, 100 or 300 Torr. In each series $\Phi(SO_2)$ and $\Phi(H_2)$ were independent of irradiation time from 300 to 900 s. In all four series $\Phi(SO_2) + \Phi(H_2) = 0.95 \pm 0.06$. However, $\Phi(SO_2)$ increased and $\Phi(H_2)$ decreased as the O_2 pressure was raised.

For a series of runs with $[CH_3SH] = 25.6 \pm 0.1$ Torr and $[O_2] = 25.9$ Torr the absorbed intensity was varied from 0.15 to 2.3 mTorr s^{-1}; this had no effect on $\Phi\{(CH_3S)_2\}$ and $\Phi(C_3H_8S_2)$, and only a slight effect on $\Phi(SO_2)$ and $\Phi(H_2)$.

In order to test for an inert gas effect, nitrogen was added in a series of runs. The effect of added nitrogen on the photo-oxidation of CH_3SH is shown in Table 3. There is no trend for $\Phi(SO_2)$ or $\Phi(H_2)$ and their sum remains at 0.92 ± 0.03. There is a very slight increase in $\Phi\{(CH_3S)_2\}$ and a factor of 2.5 decrease in $\Phi(C_3H_8S_2)$ as the nitrogen pressure increases from 0 to 262 Torr.

Two series of runs were done at 10.6 ± 0.9 and 23.6 ± 2.4 Torr O_2 to see the effect of CH_3SH pressure on the photo-oxidation of CH_3SH. Varying

TABLE 3

Effect of nitrogen on the photo-oxidation of CH_3SH

$[N_2]$ (Torr)	Irradiation time (s)	$\Phi\{(CH_3S)_2\}$	$\Phi(C_3H_8S_2)$	$\Phi(H_2S)$	$\Phi(SO_2)$[a]	$\Phi(H_2)$	$\Phi(SO_2) + \Phi(H_2)$
$[CH_3SH] = 10.44 \pm 0.23$ Torr; $[O_2] = 10.35 \pm 0.39$ Torr; $[Ar] = 15.8 \pm 0.2$ Torr; $I_a = 0.96 \pm 0.02$ mTorr s^{-1}							
0[b]	655	0.90	0.076	—	0.110	0.87	0.98
50	645	1.07	0.060	—	0.081	0.83	0.91
101	555	1.20	0.035	—	0.086	0.84	0.93
262	690	1.29	0.029	—	0.116	0.76	0.87
$[CH_3SH] = 19.8 \pm 0.4$ Torr; $[O_2] = 19.6 \pm 1.9$ Torr; $[Ar] = 16.1 \pm 0.4$ Torr; $I_a = 1.18 \pm 0.02$ mTorr s^{-1}							
0	600	1.18	0.079	0.100	0.082	0.88	0.96
53	660	1.18	0.055	0.067	0.085	0.81	0.90
106	600	1.27	0.074	0.050	0.096	0.82	0.92
302	600	1.58	0.132	0.032	0.110	0.76	0.87
$[CH_3SH] = 20.1 \pm 0.5$ Torr; $[O_2] = 101 \pm 1$ Torr; $[Ar] = 16.0 \pm 0.5$ Torr; $I_a = 1.21 \pm 0.03$ mTorr s^{-1}							
0	300	—	—	0.017	0.32	0.64	0.96
100	600	—	—	0.010	0.38	0.49	0.87
300	610	—	—	0.004	0.40	0.42	0.82
660	600	—	—	0.003	0.44	0.31	0.75

[a] Analysis of SO_2 by gas chromatography.
[b] $[CH_3SH] = 9.00$ Torr; $[Ar] = 22.8$ Torr; $I_a = 0.82$ mTorr s^{-1}.

the CH_3SH pressure from 2.0 to 63 Torr had no effect on $\Phi\{(CH_3S)_2\}$, $\Phi(C_3H_8S_2)$, $\Phi(SO_2)$ or $\Phi(H_2)$.

The effect of O_2 on the photo-oxidation of CH_3SH is given in Table 4. $\Phi\{(CH_3S)_2\}$ increases from values of less than unity at very low O_2 pressures to about 1.5 at 300 Torr O_2. The one run done with CD_3SH at 96 Torr O_2 gives $\Phi\{(CD_3S)_2\}$ = 2.06, but without more data it is difficult to know how meaningful this is. (The difference between the deuterated and protonated species may reflect different analytical sensitivities and should not be given much importance.) $\Phi(C_3H_8S_2)$ also rises with O_2 pressure from 0.07 at 1.5 Torr O_2 to about 0.4 at 300 Torr O_2. Again the one point with CD_3SH at 96 Torr O_2 gives $\Phi(C_3D_8S_2)$ greater than expected from the non-deuterated results. $\Phi(SO_2)$ increases and $\Phi(H_2)$ decreases with increasing O_2 pressure, but their sum remains 0.94 ± 0.06 except for the run with CD_3SH where the sum is 0.70.

$(CH_3S)_2$ was photo-oxidized at wavelengths above 280 nm in the presence of CH_3SH in order to produce CH_3S radicals in the absence of hydrogen atoms. The results are shown in Table 5. $\Phi(C_3H_8S_2)$ behaves in the same manner as in the photo-oxidation of CH_3SH, i.e. $\Phi(C_3H_8S_2)$ increases with O_2 pressure. However, neither SO_2 nor H_2 are produced in this system where hydrogen atoms and HO_2 radicals are absent, but they are produced in the photo-oxidation of CH_3SH where hydrogen atoms and HO_2 radicals are present. Thus these products arise exclusively from hydrogen atom and HO_2 radical reactions.

In order to obtain more mechanistic information, $(CH_3S)_2$ was photolyzed at wavelengths above 280 nm in the presence of CD_3SH. Table 6 shows the results in the absence of O_2. No H_2 or $C_3H_5D_3S_2$ are formed, but considerable exchange occurs which first produces $CH_3S_2CD_3$ and then $(CD_3S)_2$ as a secondary product. The results in the presence of O_2 are shown in Table 7. The exchange still occurs at about the same efficiency as in the absence of O_2. However, now $C_3H_5D_3S_2$ is seen, but at much lower quantum yields than those for $C_3H_8S_2$ in the fully protonated system.

4. Discussion

4.1. Photo-oxidation of $(CH_3S)_2$ in the presence of CH_3SH

SO_2 is formed when $(CH_3S)_2$ is photo-oxidized in the absence of CH_3SH [1], but not in its presence. Therefore CH_3SH must intercept the radicals that lead to SO_2 formation. Furthermore these reactions involving CH_3SH, although they do not lead to SO_2 or H_2 formation, do lead to $C_3H_8S_2$ formation and to deuterium exchange via a chain process. The exchange step is independent of both the CH_3SH and O_2 pressure. The $C_3H_8S_2$ formation is independent of CH_3SH pressure but increases with O_2 pressure from a lower limiting value of 0.03 to an upper limiting value of about 0.15.

In addition to reactions (1) - (5) the suggested reactions in the non-deuterated system are

TABLE 4

Effect of oxygen on CH_3SH photo-oxidation[a]

[O₂] (Torr)	I_a (mTorr s⁻¹)	Irradiation time (s)	Φ{(CH₃S)₂}	Φ(C₃H₈S₂)	Φ(H₂S)	Φ(SO₂)[b]	Φ(H₂)	Φ(SO₂) + Φ(H₂)
0	0.69	600	—	—	0.16	—	—	—
0	0.88	600	—	—	0.14	—	—	—
1.50	0.46	—	0.71	0.070	—	0.026	—	—
1.52	0.47	—	0.85	—	—	—	—	—
1.55	0.44	—	0.92	—	—	—	—	—
1.85	0.46	—	0.80	0.070	—	0.051	—	—
2.01	0.74	600	1.13	0.113	—	0.025[c]	0.95	0.98
6.09	0.31	—	1.02	0.018	—	—	—	—
6.19	0.31	—	1.00	0.018	—	0.026	—	—
17.7	0.69	600	—	—	0.093	—	—	—
17.7	1.21	600	1.18	0.079	0.100	0.082[c]	0.88	0.96
18.5	0.48	—	0.92	0.103	—	—	—	—
19.2	1.16	300	0.98	0.059	0.100	—	0.92	—
19.3	0.48	—	1.20	0.059	—	0.113	—	—
20.0	1.18	900	—	—	0.082	0.085[c]	0.83	0.92
20.0	0.45	—	1.27	—	—	0.082	—	—
20.0	0.52	—	1.21	0.113	—	0.122	—	—
20.7	0.72	900	—	—	0.107	—	—	—
22.0	0.87	900	—	—	0.069	—	—	—
22.3	0.81	720	1.35	0.082	—	0.054	0.81	0.86
23.0	0.46	—	1.07	0.113	—	—	—	—
24.0	1.21	1215	—	—	0.067	0.082[c]	0.76	0.84
25.1	0.46	—	1.07	—	—	0.127	—	—
27.2	0.46	—	0.98	0.121	—	0.241	—	—
61.9	0.74	300	—	—	0.027	—	—	—

(continued)

TABLE 4 *(continued)*

[O_2] (Torr)	I_a[a] (mTorr s^{-1})	Irradiation time (s)	$\Phi[(CH_3S)_2]$	$\Phi(C_3H_8S_2)$	$\Phi(H_2S)$	$\Phi(SO_2)$[b]	$\Phi(H_2)$	$\Phi(SO_2) + \Phi(H_2)$
62.2	0.71	600	—	—	0.097	—	—	—
62.6	0.72	900	—	—	0.041	—	—	—
62.7	0.73	1395	—	—	0.036	—	—	—
63.5	0.87	300	—	—	0.027	—	—	—
63.7	0.81	1200	—	—	0.040	—	—	—
66.9	1.15	300	1.15	0.130	0.038	0.181[c]	0.78	0.96
96.0[d]	1.83	550	2.06[e]	0.314[f]	—	0.224[c]	0.48	0.70
99.0	0.48	—	1.21	0.141	—	0.254	—	—
99.2	0.66	900	—	0.160	0.020	0.222	—	—
99.3	0.48	—	1.23	—	0.018	—	—	—
99.8	0.65	600	—	—	—	—	—	—
100.0	0.48	—	1.15	0.152	—	0.49	—	—
100.0	0.47	—	1.22	0.162	—	0.40	—	—
100.0	0.97	600	1.60	0.161	—	0.56[c]	0.46	1.02
100.0	0.73	630	1.81	0.181	—	0.30[c]	0.56	0.86
101.0	1.25	900	—	—	0.017	—	—	—
101.8	0.71	675	1.48	0.187	—	0.43[c]	0.59	1.02
204	1.92	585	1.38	—	—	0.65[c]	0.27	0.92
300	0.46	—	1.46	0.443	—	—	—	—
300	0.41	—	1.62	0.442	—	1.05	—	—
300	0.48	—	1.49	0.249	—	—	—	—
301	0.70	450	—	—	< 0.01	—	—	—
305	0.42	—	1.51	0.350	—	1.17	—	—
305	0.85	450	—	—	< 0.01	—	—	—

[a] [CH_3SH] = 21.0 ± 1.8 Torr; [Ar] = 15.0 ± 1.7 Torr.
[b] Analysis of SO_2 by mass spectrometry except where indicated.
[c] Analysis of SO_2 by gas chromatography.
[d] CD_3SH rather than CH_3SH.
[e] $(CD_3S)_2$ rather than $(CH_3S)_2$.
[f] $C_3D_8S_2$ rather than $C_3H_8S_2$.

TABLE 5

Photo-oxidation of $(CH_3S)_2$ in the presence of CH_3SH [a]

$[O_2]$ (Torr)	$[CH_3SH]$ (Torr)	$\Phi(C_3H_8S_2)$
2.0	20.2	0.033
9.9	19.8	0.032
16.6	10.4	0.036
19.7	19.7	0.036
21.0	2.2	0.034
23.8	60.9	0.018
48.9	19.2	0.032
51.5	18.9	0.058
98.7	25.1	0.160
105.7	19.4	0.143
306	20.0	0.214
310	61.7	0.141

[a]$[(CH_3S)_2] = 9.46 \pm 0.41$ Torr; $[Ar] = 11.5 - 18.8$ Torr; $I_a = 0.81 \pm 0.14$ mTorr s^{-1}; $\Phi(SO_2)$ and $\Phi(H_2)$ are zero (less than 0.01 in all runs).

$$CH_3S(O)_2 + CH_3SH \longrightarrow C_2H_7S_2O_2 \tag{6}$$

$$CH_3SO_4 + CH_3SH \longrightarrow C_2H_7S_2O_4 \tag{7}$$

Since there is no dependence of $\Phi(C_3H_8S_2)$ on $[CH_3SH]$, $[(CH_3S)_2]$ or I_a, reactions (6) and (7) must be so rapid that the other reaction paths involving $CH_3S(O)_2$ and CH_3SO_4 are unimportant under all the conditions studied. The adduct radicals formed in reactions (6) and (7) can react with other $CH_3S(O)_2$ or CH_3SO_4 radicals to regenerate reactants or produce $C_3H_8S_2$. At low O_2 pressures, where $CH_3S(O)_2$ is the predominant oxygenated radical, the ratio of $C_3H_8S_2$ formed to $(CH_3S)_2$ regenerated is about 0.03. At high O_2 pressures, where CH_3SO_4 is the predominant oxygenated radical, the ratio of $C_3H_8S_2$ formed to reactant regenerated is considerably higher and reaches about 0.15. With CD_3SH the formation of $C_3H_5D_3S_2$ is much less efficient than the production of $C_3H_8S_2$ in the fully protonated system.

The isotope exchange reactions can involve any of the oxygenated (or even unoxygenated) CH_3S radicals, and occur via

$$CH_3SO_x + CD_3SH \longrightarrow CD_3SO_x + CH_3SH \tag{8a}$$

$$CD_3SO_x + (CH_3S)_2 \longrightarrow CD_3SSCH_3 + CH_3SO_x \tag{9}$$

For long chains, mass balance considerations lead to

$$-\Phi\{(CH_3S)_2\} = -\Phi(CD_3SH) = \Phi(CH_3S_2CD_3) \tag{I}$$

For the data in Table 6

$$\frac{-\Phi\{(CH_3S)_2\}}{-\Phi(CD_3SH)} = 0.98 \pm 0.41$$

TABLE 6

Photolysis of $(CH_3S)_2$ in the presence of CD_3SH [a]

[CD₃SH] (Torr)	[(CH₃S)₂] (Torr)	I_a (mTorr s⁻¹)	$-\Phi\{(CH_3S)_2\}$	$-\Phi(CD_3SH)$	$\Phi(CH_3S_2CD_3)$	$k_9/k_5^{1/2} \times 10^7$ ((cm³ s⁻¹)^{1/2})
2.1	9.4	0.67	9.0	4.6	11.4	1.74
10.8	9.1	0.65	7.8	6.3	11.2	1.74
16.2	8.7	0.73	3.1	6.2	6.2	1.06
20.5	1.17	0.083	8.4	12.0	5.8	2.50
20.8	5.2	0.38	14.3	15.2	17.6	3.65
48.8	9.4	0.73	11.0	20.4	16.8	2.67

[a] $[Ar] = 15.2 \pm 1.3$ Torr; $\Phi(C_3H_5D_3S_2) < 0.001$; $\Phi(H_2) < 0.01$; $(CD_3S)_2$ is seen as a secondary product.

TABLE 7

Photo-oxidation of $(CH_3S)_2$ in the presence of CD_3SH [a]

$[O_2]$ (Torr)	$[CD_3SH]$ (Torr)	$-\Phi\{(CH_3S)_2\}$	$-\Phi(CD_3SH)$	$\Phi(CH_3S_2CD_3)$	$\Phi(C_3H_5D_3S_2)$
2.2	19.6	8.8	8.8	7.0	0.008
10.4	20.9	6.2	4.5	4.9	0.008
15.6[b]	20.4	4.1	9.4	5.4	< 0.003
19.8	54.4	7.8	9.4	5.4	0.036
21.0	1.04	1.65	0.84	1.16	0.033
53.0	19.0	5.8	—	7.4	0.015
63.6	21.0	3.6	2.7	4.9	0.018
103.2	18.3	8.9	9.2	10.6	0.029

[a] $[(CH_3S)_2] = 9.6 \pm 0.7$ Torr; $[Ar] = 14.9 \pm 1.5$ Torr; $I_a = 0.72 \pm 0.06$ mTorr s^{-1}; $\Phi(SO_2)$ and $\Phi(H_2)$ are zero (less than 0.01); $(CD_3S)_2$ is seen as a secondary product.
[b] $[(CH_3S)_2] = 1.05$ Torr; $I_a = 0.075$ mTorr s^{-1}.

$$\frac{-\Phi\{(CH_3S)_2\}}{\Phi(CH_3S_2CD_3)} = 0.82 \pm 0.21$$

and

$$\frac{-\Phi(CD_3SH)}{\Phi(CH_3S_2CD_3)} = 1.02 \pm 0.42$$

For the data in Table 7

$$\frac{-\Phi\{(CH_3S)_2\}}{-\Phi(CD_3SH)} = 1.01 \pm 0.38$$

$$\frac{-\Phi\{(CH_3S)_2\}}{\Phi(CH_3S_2CD_3)} = 1.21 \pm 0.33$$

and

$$\frac{-\Phi(CD_3SH)}{\Phi(CH_3S_2CD_3)} = 1.11 \pm 0.40$$

The uncertainties are mean deviations. They are very large because it is difficult to obtain loss yields with an accuracy to better than a factor of 2. Within the large uncertainties the ratios all have values of unity as required by eqn. (I).

In the absence of O_2 termination can occur via

$$2CH_3S \longrightarrow (CH_3S)_2 \tag{10}$$

$$2CD_3S \longrightarrow (CD_3S)_2 \tag{11}$$

$$CH_3S + CD_3S \longrightarrow CH_3S_2CD_3 \tag{12}$$

At low CD_3SH pressures, termination will be mainly by reaction (10), and the rate law for $CH_3S_2CD_3$ formation becomes

$$\Phi(CD_3S_2CH_3) = \frac{k_{8a}}{k_{10}^{1/2}} \frac{[CD_3SH]}{I_a^{1/2}} \qquad (II)$$

where $x = 0$ for reaction (8a). At high CD_3SH pressures termination will be mainly by reaction (11), and the rate law for $CH_3S_2CH_3$ formation becomes

$$\Phi(CD_3S_2CH_3) = \frac{k_9}{k_{11}^{1/2}} \frac{[(CH_3S)_2]}{I_a^{1/2}} \qquad (III)$$

where $x = 0$ for reaction (9). The data in Table 6 show no systematic variation of $\Phi(CD_3S_2CH_3)$ with $[CD_3SH]$; the system is always in the high pressure regime and yields $k_9/k_{11}^{1/2} = (2.2 \pm 0.7) \times 10^{-7}$ $(cm^3\ s^{-1})^{1/2}$.

In the presence of O_2, termination can occur by

$$CH_3SO_x + CD_3SH \longrightarrow termination \qquad (8b)$$

$$CD_3SO_x + CD_3SH \longrightarrow termination \qquad (13)$$

Reaction (13) is less important than reaction (8b) since the chains are long and CD_3SO_x is effectively removed by reaction (9). Thus

$$\Phi(CH_3S_2CD_3) = \frac{k_{8a}}{k_{8b}} \qquad (IV)$$

The data in Table 7 show that, except at 1.0 Torr CD_3SH, $\Phi(CH_3S_2CD_3)$ is independent of all variables. Equation (IV) gives $k_{8a}/k_{8b} = 6.5 \pm 1.6$. At 1.00 Torr CD_3SH, the CD_3SH pressure is so low that termination can occur by reactions (2) or (5) which would reduce the value of $\Phi(CH_3S_2CD_3)$.

4.2. Photolysis of CH_3SH

The photolysis of CH_3SH at 254 nm in the absence of O_2 was first studied in detail by Inaba and Darwent [6]. They found H_2 and CH_4 as products. The H_2 yield was constant and unaffected by irradiation time. However, the CH_4 yield decreased with increasing reaction time in some experiments but increased with reaction time in other experiments. Our results in Table 1 show that both $\Phi(CH_4)$ and $\Phi(H_2S)$ are unaffected by changing the reaction time and thus these products are primary.

Steer and Knight [5] studied the photolysis at 254 nm and found that $\Phi(H_2) = 1.00 \pm 0.05$ independent of pressure. This agrees with our result of 1.00 ± 0.03 independent of pressure. They also found that CF_4 quenches $\Phi(CH_4)$ from 0.19 in its absence to zero at high CF_4 pressure. Again our results confirm these findings.

However, Bridges and White [4] found that $\Phi(H_2) = 0.83 \pm 0.03$, $\Phi\{(CH_3S)_2\} = 0.99 \pm 0.1$ and $\Phi(CH_4) = 0.16 \pm 0.03$ independent of CH_3SH pressure. Like us they also found $\Phi(H_2S) = \Phi(CH_4)$. In the presence of n-C_4H_{10}, $\Phi(CH_4)$ was reduced and $\Phi(H_2)$ increased toward unity.

The only discrepancy among these findings is whether $\Phi(H_2) = 0.83$ or 1.00 at low pressure. The result of Bridges and White that $\Phi(H_2) = 0.83$ at low pressure (*i.e.* $\Phi(H_2) + \Phi(CH_4) = 1.0$ under all conditions) seems to make more sense, and we accept their finding. Bridges and White interpreted their results in terms of a hot hydrogen atom mechanism

$$CH_3SH + h\nu \longrightarrow CH_3S + H^* \tag{14a}$$

$$H^* + CH_3SH \longrightarrow H_2 + CH_3S \tag{15a}$$

$$\longrightarrow H_2S + CH_3 \tag{15b}$$

$$H^* + M \longrightarrow H + M \tag{16}$$

$$H + CH_3SH \longrightarrow H_2 + CH_3S \tag{17}$$

$$CH_3 + CH_3SH \longrightarrow CH_4 + CH_3S \tag{18}$$

$$2CH_3S \longrightarrow (CH_3S)_2 \tag{10}$$

where M in reaction (16) is any gas other than CH_3SH.

Bridges and White also considered that the primary process

$$CH_3SH + h\nu \longrightarrow CH_3 + SH \tag{14b}$$
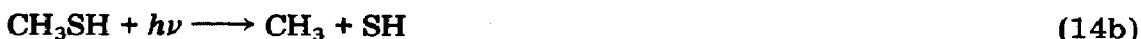
could occur with a yield of 0.07 to account for the fact that $n\text{-}C_4H_{10}$ did not quench $\Phi(CH_4)$ to zero. There is some evidence for this reaction from our work also as $\Phi(H_2S)$ appears to level off at 0.08. However, the fact that it has been found both by Steer and Knight [5] and in our work that $\Phi(CH_4)$ could be pressure quenched to zero rules against reaction (14b). Our results obtained in the presence of O_2 indicate that nitrogen can pressure quench $\Phi(H_2S)$ to zero. Thus most of the data indicate that reaction (14b) is not needed, and for simplicity we ignore it.

The reaction mechanism, neglecting reaction (14b), yields rate laws which are consistent with the results in the absence of O_2. However, in the presence of O_2, it predicts values for $\Phi(H_2)$ which are larger than those observed. Thus we have to modify the mechanism by deleting reaction (15a) and adding another primary process

$$CH_3SH + h\nu \longrightarrow CH_3S + H \tag{14c}$$

The mechanism consisting of reactions (14a), (14c), (15b), (10) and (16) - (18) gives the rate laws

$$\Phi((CH_3S)_2) = 1.0 \tag{V}$$

$$\Phi(H_2) = \phi_{14c} + \frac{k_{16}[M]}{k_{15b}[CH_3SH] + k_{16}[M]} \tag{VI}$$

$$\Phi(H_2S)^{-1} = \Phi(CH_4)^{-1} = \phi_{14a}^{-1}\left(1 + \frac{k_{16}[M]}{k_{15b}[CH_3SH]}\right) \tag{VII}$$
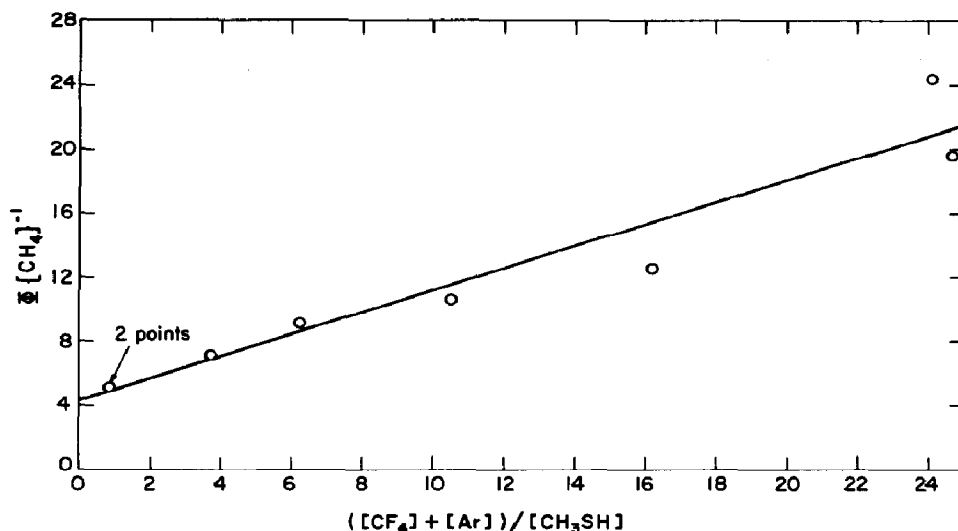
Fig. 2. Plot of $\Phi(CH_4)^{-1}$ vs. $([CF_4] + [Ar])/[CH_3SH]$ in the photolysis of CH_3SH for $[CH_3SH] = 20.4 \pm 0.7$ Torr and $[Ar] = 15.0 \pm 2.3$ Torr.

Equation (VI) predicts that $\Phi(H_2)$ will increase from $\phi_{14c} = 0.83$ at low [M] to $\phi_{14c} = 1.0$ at high [M]. In the absence of foreign gas eqn. (VII) predicts that $\Phi(H_2S) = \Phi(CH_4)$ will be 0.18 ± 0.01 from our data, 0.19 from the data of Steer and Knight [5] and 0.16 ± 0.03 from the data of Bridges and White [4].

Figure 2 is a plot of $\Phi(CH_4)^{-1}$ versus $([CF_4] + [Ar])/[CH_3SH]$ in the absence of O_2. The data fit a straight line which gives an intercept of 4.3 ± 1.1 and a slope of 0.68 ± 0.08, where the uncertainties are one standard deviation. The ratio of slope to intercept gives $k_{16}/k_{15b} = 0.157 \pm 0.056$.

The data for $\Phi(H_2S)$ do not quench to zero as nitrogen is added in the absence of O_2, but they do quench to zero in the presence of O_2. We consider the failure to quench completely in the absence of O_2 to be an experimental artifact. The appropriate quenching plots in the presence of O_2 are shown in Figs. 3 and 4. With 19.6 Torr O_2, the data in Fig. 3 fit a straight line which gives an intercept of 11.3 ± 1.1 and a slope of 1.32 ± 0.14. The ratio of slope to intercept gives a value of k_{16}/k_{15b} of 0.117 ± 0.022. With 101 Torr O_2, the data in Fig. 4 fit a straight line which gives an intercept of 70 ± 28 and a slope of 8.8 ± 1.6. The ratio of slope to intercept gives a value for k_{16}/k_{15b} of 0.125 ± 0.068 in excellent agreement with the value obtained at 19.6 Torr O_2. These values are slightly less than those obtained for k_{16}/k_{15b} from Fig. 2, which indicates that the quenching efficiency of nitrogen is a factor of 0.77 of that of CF_4.

4.3. Photo-oxidation of CH₃SH

When CH_3SH is photo-oxidized, the products are H_2, SO_2, H_2S, $C_3H_8S_2$ and $(CH_3S)_2$, but not CH_4. The SO_2 must come from hydrogen atoms or
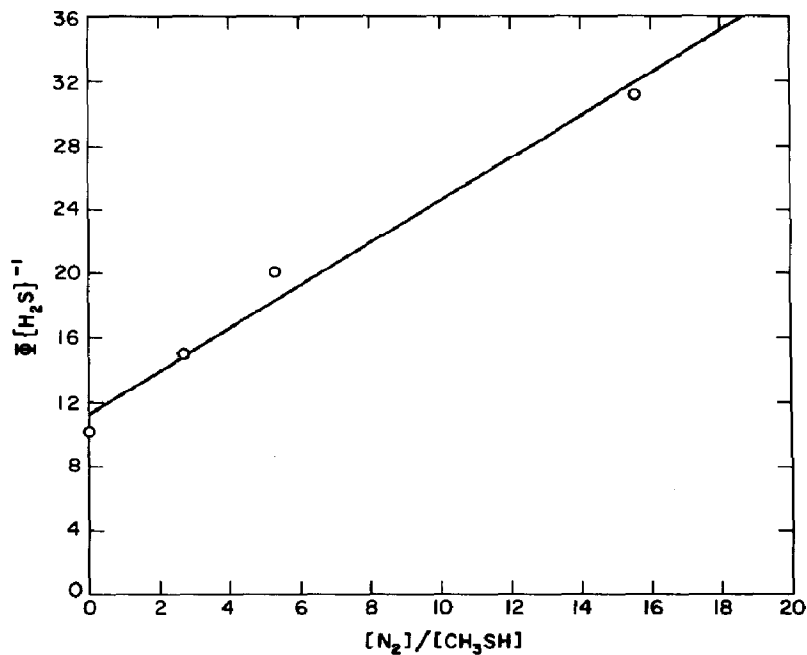
Fig. 3. Plot of $\Phi(H_2S)^{-1}$ vs. $[N_2]/[CH_3SH]$ in the photo-oxidation of CH_3SH for $[CH_3SH] = 19.8 \pm 0.4$ Torr, $[O_2] = 19.6 \pm 1.9$ Torr, $[Ar] = 16.1 \pm 0.4$ Torr and $I_a = 1.18 \pm 0.02$ mTorr s^{-1}.
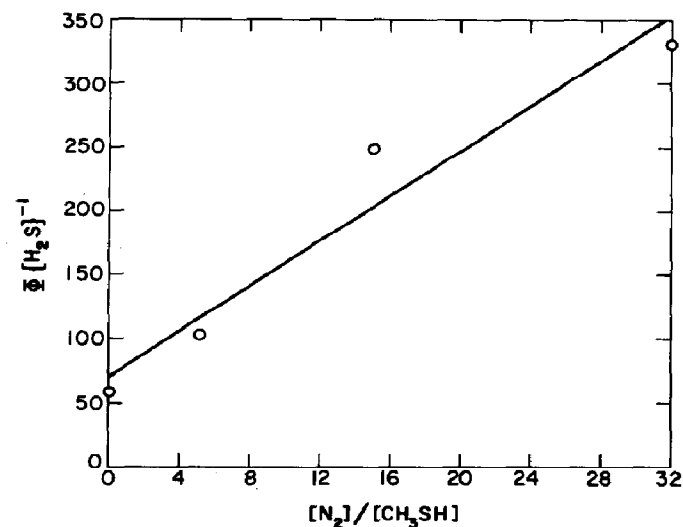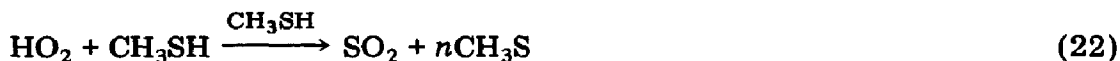

Fig. 4. Plot of $\Phi(H_2S)^{-1}$ vs. $[N_2]/[CH_3SH]$ in the photo-oxidation of CH_3SH for $[CH_3SH] = 20.1 \pm 0.5$ Torr, $[O_2] = 101 \pm 1$ Torr, $[Ar] = 16.0 \pm 0.5$ Torr and $I_a = 1.21 \pm 0.03$ mTorr s^{-1}.

CH_3 radicals as precursors, as it is not formed in the photo-oxidation of $(CH_3S)_2$ in the presence of CH_3SH. The necessary additional reactions are

$$CH_3 + O_2 + M \longrightarrow CH_3O_2 + M \qquad (19)$$

$$H + O_2 + M \longrightarrow HO_2 + M \tag{20}$$

$$CH_3O_2 + CH_3SH \xrightarrow{CH_3SH} SO_2 + nCH_3S \tag{21}$$

$$HO_2 + CH_3SH \xrightarrow{CH_3SH} SO_2 + nCH_3S \tag{22}$$

where reactions (21) and (22) represent some overall reactions which lead to SO$_2$ production. They are branched-chain reactions needed to account for the fact that $\Phi\{(CH_3S)_2\}$ can exceed unity. For simplicity the value of n is assumed to be the same in both reactions.

The mechanism now consists of reactions (14a), (14c), (15b), (16), (17), (19) - (22), (1) - (3), (6) and (7). The fact that CH$_4$ is not formed indicates that reaction (18) is negligible compared with reaction (19). This mechanism leads to the rate laws

$$\frac{\phi_{14c} + \alpha\phi_{14a}}{\Phi(H_2)} = 1 + \frac{k_{20}[O_2][M]}{k_{17}[CH_3SH]} \tag{VIII}$$

$$\frac{\phi_{1c} + \alpha\phi_{14a}}{\Phi(SO_2) - (1 - \alpha)\phi_{14a}} = 1 + \frac{k_{17}[CH_3SH]}{k_{20}[O_2][M]} \tag{IX}$$

$$\frac{\Phi(SO_2) - (1 - \alpha)\phi_{14a}}{\Phi(H_2)} = \frac{k_{20}[O_2][M]}{k_{17}[CH_3SH]} \tag{X}$$

where [M] is taken to be [N$_2$] + [Ar] + [O$_2$] + 3[CH$_3$SH]. The quantity α is

$$\alpha \equiv \frac{k_{16}[M]}{k_{15b}[CH_3SH] + k_{16}[M]}$$

where here [M] = [N$_2$] + [Ar] + [O$_2$]. The quantity α can be computed for each run from the values of k_{16}/k_{15b} reported above. Thus the left-hand sides of each equation can be computed for each run and plotted against the appropriate reactant pressure ratios.

Figure 5 is a plot of the left-hand side of eqn. (VIII) *versus* [O$_2$][M]/ [CH$_3$SH]. The plot gives a good straight line with an intercept of 0.85 ± 0.05 and a slope of $(9.09 \pm 0.27) \times 10^{-4}$ Torr^{-1}. The intercept should be unity; thus the value of 0.85 indicates a consistent error in the H$_2$ determinations. The ratio of slope to intercept gives $k_{20}/k_{17} = (1.07 \pm 0.09) \times 10^{-3}$ Torr^{-1}.

Figure 6 is a plot of the left-hand side of eqn. (IX) *versus* [CH$_3$SH]/ [O$_2$][M]. For this plot the data are very scattered because the denominator of the left-hand side of eqn. (IX) is the difference of two similar numbers. Only values in which $\Phi(SO_2) - (1 - \alpha)\phi_{14c}$ were 0.10 or more were used to minimize the scatter. The least-squares straight line gives an intercept of 1.66 ± 0.25 and a slope of $(1.11 \pm 0.12) \times 10^3$ Torr. The intercept is considerably larger than unity and reflects the large error in computing the left-
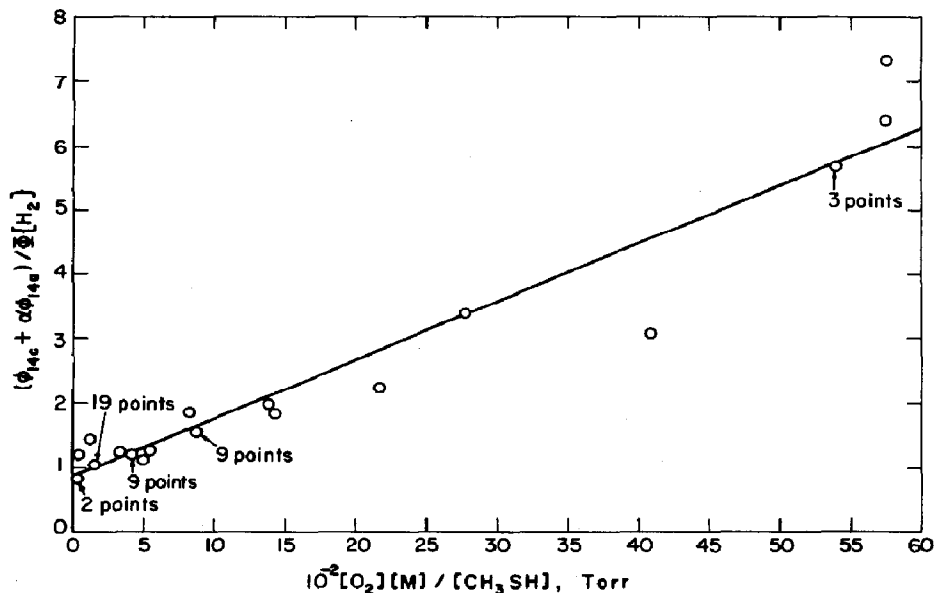
Fig. 5. Plot of $(\phi_{14c} + \alpha\phi_{14a})/\Phi(H_2)$ vs. $[O_2][M]/[CH_3SH]$ in the photo-oxidation of CH_3SH.
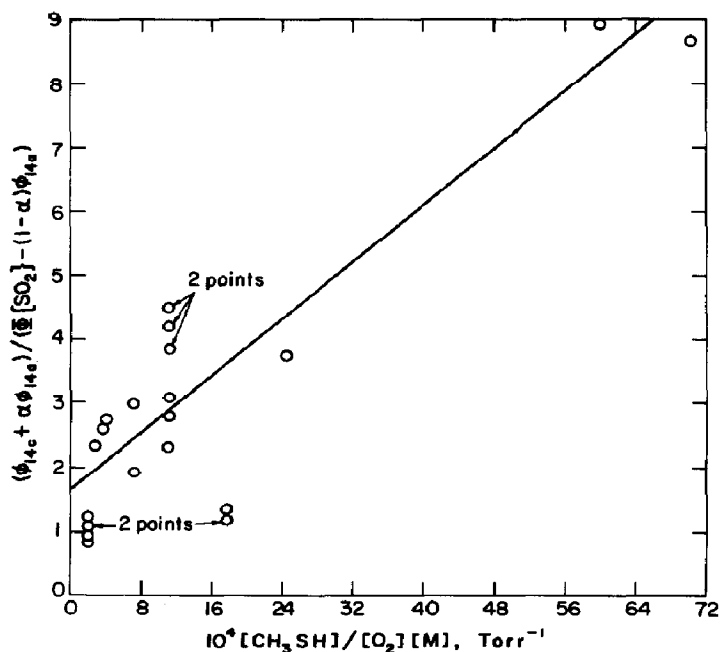

Fig. 6. Plot of $(\phi_{14c} + \alpha\phi_{14a})/\{\Phi(SO_2) - (1 - \alpha)\phi_{14a}\}$ vs. $[CH_3SH]/[O_2][M]$ in the photo-oxidation of CH_3SH.

hand side of eqn. (IX). However, the slope gives $k_{20}/k_{17} = (0.90 \pm 0.10) \times 10^{-3}$ Torr^{-1} in good agreement with the value obtained from eqn. (VIII) and Fig. 5. The ratio of intercept to slope gives a value for k_{20}/k_{17} of (1.50 ±

0.35) $\times 10^{-3}$ Torr^{-1}, which is also in good agreement with that obtained from eqn. (VIII) and Fig. 5.

Equation (X) is a combination of eqns. (VIII) and (IX) and permits the evaluation of k_{20}/k_{17} over a much larger range of the variables. Figure 7 is a log–log plot of the left-hand side of eqn. (X) *versus* $[O_2][M]/[CH_3SH]$. The data are fitted by a least-squares line of slope 1.0 and give $k_{20}/k_{17} = (0.59 \pm 0.26) \times 10^{-3}$ Torr^{-1}, which is about a factor of 2 lower than that obtained from Figs. 5 or 6.

The literature value for k_{20} is $(5.5 \pm 0.5) \times 10^{-32}$ cm^6 s^{-1} at 300 K with nitrogen as a chaperone [7]. Taking k_{17}/k_{20} as 1000 Torr gives $k_{17} = 1.8 \times 10^{-12}$ cm^3 s^{-1}. In part I of this series we reported $k_{17} = 4.1 \times 10^{-13}$ cm^3 s^{-1} based on the competition for hydrogen atoms between NO and CH$_3$SH [2]. These two values have a discrepancy of a factor of 4.4. However, the value obtained by the competition for hydrogen atoms between CH$_3$SH and NO assumed a rate coefficient for the H + NO + M reaction based on argon as a chaperone and equal efficiencies for argon and NO. For the H + O$_2$ + M reaction O$_2$ is 3.4 times as efficient as argon [7]. If this same efficiency factor applies to the H + NO + M reaction then the earlier determination for k_{17} should be raised to 1.4×10^{-12} cm^3 s^{-1} which is in good agreement with the value of 1.8×10^{-12} cm^3 s^{-1} obtained in this study. Furthermore the value of k_{17} obtained in the earlier study was based on an analysis that neglected reaction (14c). A reanalysis of the data with reaction (14c)
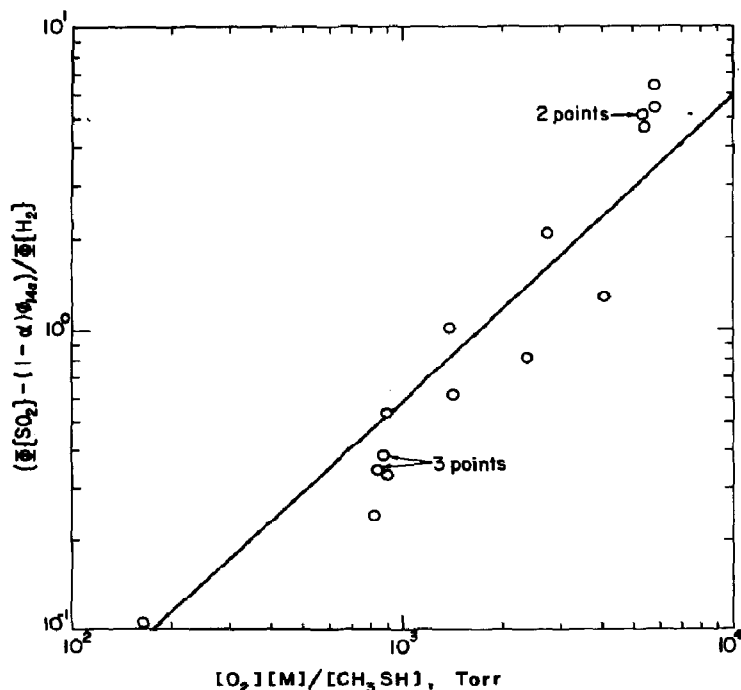

Fig. 7. Log–log plot of $\{\Phi(SO_2) - (1 - \alpha)\phi_{14a}\}/\Phi(H_2)$ *vs.* $[O_2][M]/[CH_3SH]$ in the photo-oxidation of CH$_3$SH.
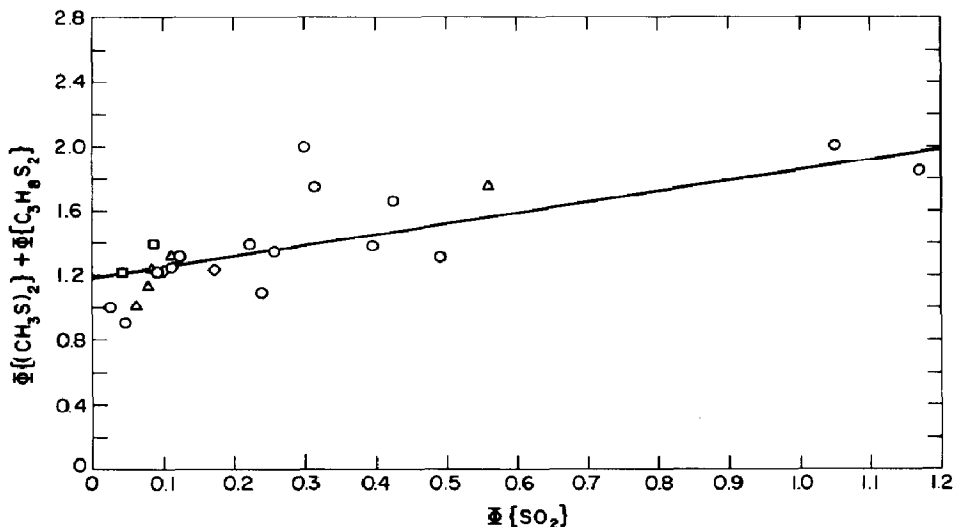
Fig. 8. Plot of $\Phi\{(CH_3S)_2\} + \Phi(C_3H_8S_2)$ vs. $\Phi(SO_2)$ in the photo-oxidation of CH_3SH: ◇, 2 Torr CH_3SH; △, 10 Torr CH_3SH; ○, 20 Torr CH_3SH; ▢, 60 Torr CH_3SH.

included raises k_{17} by 71% to 2.4×10^{-12} cm^3 s^{-1} [8]. This value is still in reasonable agreement with that obtained in this study.

In addition to eqns. (II) - (IV) the mechanism also predicts

$$\Phi(H_2) + \Phi(SO_2) = 1.0 \tag{XI}$$

Values of $\Phi(H_2) + \Phi(SO_2)$ are tabulated in Tables 3 and 4 and it can be seen that eqn. (XI) is satisfied to within the experimental uncertainty of the data.

The mechanism also predicts

$$\Phi(C_3H_8S_2) + \Phi\{(CH_3S)_2\} \approx 1.0 + \frac{n-1}{2}\,\Phi(SO_2) \tag{XII}$$

Figure 8 is a plot of the left-hand side of eqn. (XII) versus $\Phi(SO_2)$. The data are very scattered, but the least-squares straight line gives

$$\Phi(C_3H_8S_2) + \Phi\{(CH_3S)_2\} = 1.19 \pm 0.06 + (0.70 \pm 0.14)\,\Phi(SO_2) \tag{XIII}$$

The ratio of slope to intercept is 0.58 ± 0.14 which gives $n = 2.16 \pm 0.28$.

We do not understand the detailed mechanism by which $C_3H_8S_2$ is formed from the $C_2H_7S_2O_2$ and $C_2H_7S_2O_4$ radicals produced in reactions (6) and (7) respectively. Neither do we have any idea how the SO_2-forming steps (reactions (21) and (22)) occur. All these processes may be heterogeneous.

Acknowledgments

332

References

1 R. J. Balla and J. Heicklen, *J. Photochem.*, *29* (1985) 297 - 310.
2 R. J. Balla and J. Heicklen, *Can. J. Chem.*, *62* (1984) 162.
3 R. J. Balla and J. Heicklen, *J. Phys. Chem.*, *88* (1984) 6314.
4 L. Bridges and J. M. White, *J. Phys. Chem.*, *77* (1973) 295.
5 R. P. Steer and A. R. Knight, *J. Phys. Chem.*, *72* (1968) 2145.
6 T. Inaba and B. de B. Darwent, *J. Phys. Chem.*, *64* (1960) 1431.
7 R. F. Hampson, Chemical kinetics and photochemical data sheets for atmospheric reactions, *Rep. FAA-EE-80-17*, 1980 (U.S. Department of Transportation).
8 R. J. Balla, *Ph.D. Thesis*, Pennsylvania State University, 1984.